J Nanopart Res (2017) 19: 329
DOI 10.1007/s11051-017-4018-0

RESEARCH PAPER

Induction of cell death by magnetic particles in response to a gradient magnetic field inside a uniform magnetic field

Carlos David Amaya-Jaramillo · Adriana Patricia Pérez-Portilla · José Javier Serrano-Olmedo · Milagros Ramos-Gómez

Received: 13 March 2017 / Accepted: 7 September 2017 / Published online: 26 September 2017

Abstract A new instrument based on a magnetic force produced by an alternating magnetic field gradient, which is obtained through Maxwell coils, inside a constant field magnet has been designed and used to produce cell death. We have determined the interaction of microparticles and cells under different conditions such as incubation time with microparticles, particle size, magnetic field exposition time, and different current waveforms at different frequencies to produce a magnetic field gradient. We determined that the highest rate of cell death occurs at a frequency of 1 Hz with a square waveform and 1 h of irradiation. This method could be of great interest to remove cancer cells due mainly to the alterations in stiffness observed in the membranes of the tumor cells. Cancer cells can be eliminated in response to the forces caused by the movement of magnetic nanoparticles of the appropriate size under the application of a specific magnetic field.

Keywords Gradient magnetic field · Magnetic microparticles · Microparticles motion · Cell death · Lysosomes · Nanomedicine

Abbreviations

μ	Permeability of medium
V	Volume of the MMPs
H_y	Magnetic field y-component strength
χ	Susceptibility of the MMPs
$\vec{m}$	Magnetic moment
$\vec{B}_{ext}$	Magnetic external field

Introduction

Magnetic nanoparticles (MNPs) and magnetic microparticles (MMPs) have attracted a lot of research interest, especially in biomedicine, where their main applications are drug delivery, hyperthermia induction, and as a contrast agent in magnetic resonance imaging (MRI) (Hernando Grande 2007). Current efforts in research on nanoparticles for biomedical applications are aimed at achieving less invasive procedures that cause fewer traumas during patient treatment.

As mentioned, there have been many efforts to produce cancer cell death by MNPs especially using high-frequency coils (Hergt et al. 2006; Kumar and Mohammad 2011; Serantes et al. 2014; Golovin et al.

Electronic supplementary material The online version of this article (https://doi.org/10.1007/s11051-017-4018-0) contains supplementary material, which is available to authorized users.

C. D. Amaya-Jaramillo · J. J. Serrano-Olmedo · M. Ramos-Gómez (✉)
Centre for Biomedical Technology (CTB), Universidad Politécnica de Madrid (UPM), Madrid, Spain
e-mail: milagros.ramos@ctb.upm.es

A. P. Pérez-Portilla
Department of Immunology and Oncology, Centro Nacional de Biotecnología/Consejo Superior de Investigaciones Científicas (CNB-CSIC), Madrid, Spain

J. J. Serrano-Olmedo · M. Ramos-Gómez
CIBER de Bioingeniería, Biomateriales y Nanomedicina (CIBER-BBN), Madrid, Spain

2015), or by using a remote dynamic magnetic field (dmf) that rotates the MNPs, causing cell death by apoptosis (Zhang et al. 2014; Cheng et al. 2016). This work is intended to make the MMPs, which are subject to a magnetic field gradient within a uniform magnetic field, can cause cell death.

All materials have specific characteristics produced by a magnetic field, and MMPs have ferromagnetism, which is a physical phenomenon of magnetic ordering of all magnetic moments in a sample in the same direction and sense. In this context, small-sized MMPs require a high magnetic field to induce their motion due to their low magnetization and their interactions with the fluids that cause Brownian motions (Dobson 2006). Therefore, a magnetic field is not large enough to control the movement of MMPs because the magnetic field creates MMP clusters (Zhang et al. 2014). However, it is possible to control the movement of MMPs by a gradient magnetic field where a large uniform magnetic field magnetizes the MMPs and a magnetic gradient determines the direction of movement.

In this work, we demonstrate that induction of a linear motion in MMPs can be used to induce cell death. We show that MMPs internalized in lysosomes produce damage to the cell membrane that eventually causes cell death in response to the application of a magnetic field.

Material and methods

We have designed and built an experimental setup from a combination of a constant magnetic field of 100 mT and a homogeneous gradient magnetic field that varies over time to produce a periodic motion (Fig. 1 and Movie 1).

Magnetic particle selection

The greater the particle mass, the higher the linear momentum it acquires, and mechanical interaction with cells occurs because the magnetic force experienced by a dipole is:

$$\vec{F}_{magnetic} = \nabla\left(\vec{m}\cdot\vec{B}_{ext}\right) \quad (1)$$

which depends on the volume of the magnetic material (Jiles 1998; Serantes et al. 2014) and that interaction can produce cell damage. Large-sized MMPs (> 10 μm) can only cause displacement of the cells, since rapid movements of the MMPs are not easily achieved within a viscous fluid such as intracellular medium (Sanchez et al. 2011). However, small particles (< 500 nm) may be too small to generate enough force to produce the membrane rupture and their interaction with cells would simply puncture the lysosome membrane without causing enough damage to produce cell death. Therefore, particles should have a size similar to that used in the biolistic transformation process to produce damage to cell membranes (Frame et al. 2000). We used spherical MMPs in this study to know the interaction between MMPs and cells in our equipment. These MMPs have magnetic isotropy so their position in their environment is negligible. So, we worked with particles with diameters of 300 nm (ChemicellfluidMAG-ARA 4115), 500 nm (ChemicellfluidMAG-PVA 4120), and 2 μm (ChemicellSiMAG/MP-DNA 1102). These particles were selected because their cores are of magnetite, and its coating is of biocompatible material as the manufacturer indicates it. In addition, for more information on the magnetic characteristics of the MNPs and MMPs, we have used an alternating gradient field magnetometer (AGFM), MicroMag ™ 2900 AGM System to obtain the hysteresis loops of the MNPs and MMPs chosen in this work.

Magnetic arrangement

It is possible to produce the movement of the MNPs through a specially designed magnetic arrangement (Dobson 2006).

We developed and constructed an equipment, which is mostly one-dimensional (Fig. 1), where the uniform constant magnetic field has only one dimension in the y-coordinate so that it satisfies Eq. 2.

$$\vec{F}_{magnetic} = \mu\vec{m}\frac{\partial\vec{H}}{\partial y} = \mu\chi V H_y\frac{\partial\vec{H}}{\partial y} \quad (2)$$

The instrument is built so that each coil has the same amplitude of current flow in the opposite direction to the other coil; a gradient is formed in the volume between them (Fig. 2). Additional data are given in Online Resource 1.

Temperature control

To maintain stable conditions in the samples, we have made a device in which water preheated to 30 °C flows

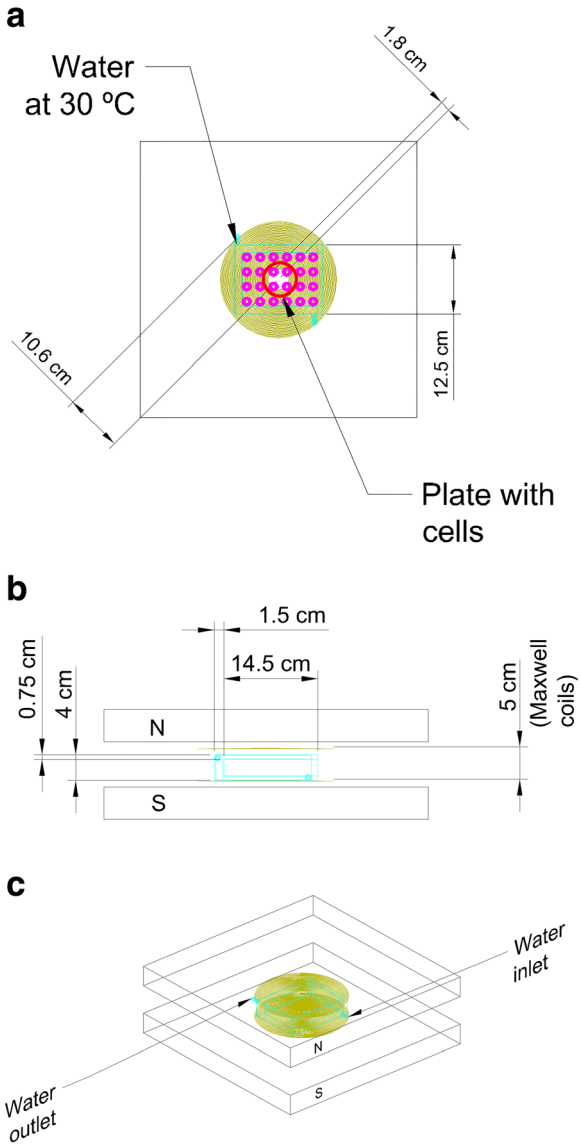

Fig. 1 Magnetic arrangement: Maxwell coils and permanent magnet (100 mT). The cell culture plate (P24 multiwell) was maintained under stable conditions by a flow of water at 30 °C. **a** Top view, where the P24 multiwell (purple color) is inside the water jacket (cyan color). Only wells inside the red circle are used in this work. **b** Front view of the equipment with its dimensions. **c** Isometric view, where the arrows indicate the water inlet and outlet in the water jacket

continuously around the P24 multiwell, where the cells are plated.

To measure the temperature, we placed the P24 plate containing water and MMPs at 0.05 mg/ml in separate wells, inside the device. The P24 was then subjected to the gradient magnetic field and constant magnetic field for 120 min at 1 Hz with a square-shaped current of 7 A

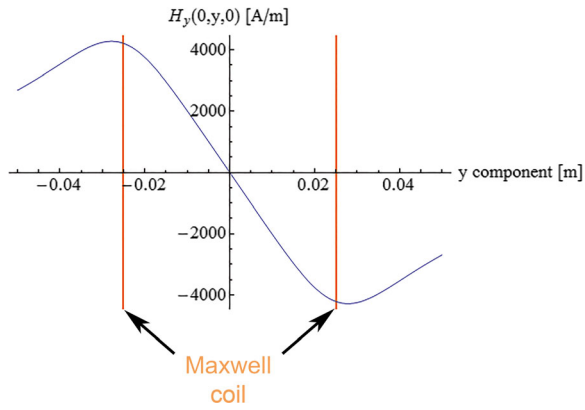

Fig. 2 Magnetic field strength with a current of 7 A amplitude produced by the Maxwell coils (orange), without the contribution of the permanent field

from 28 °C. The temperature was measured with a Fluoroptic thermometer (Luxtronm3300) placed inside the P24 wells.

Cell culture

Mouse fibroblastic cells (NIH/3T3; ATCC NCRL-1658) were maintained in Dulbecco's Modified Eagle Medium (DMEM), supplemented with 5% heat-inactivated fetal bovine serum, 2 mM of L-glutamine, 0.1 mM of nonessential amino acids, 100 U/ml of penicillin, and 100 mg/ml of streptomycin (Life Technologies). The cell line was maintained at 37 °C in a humidified incubator of 5% CO_2 and 95% air and passaged twice per week.

Cell viability

Cell viability after magnetic field application was evaluated by lactate dehydrogenase (LDH) activity assay. The assay is based on the measurement of LDH enzyme released into the cell culture medium when damage to the plasma membrane occurs and the integrity of the cell membrane is lost. Cells were seeded at an initial density of 2.5×10^4 cells/cm^2 in 24-well plates. Cell cultures were incubated for 24 h with particles of different sizes (2 μm, 500 nm, and 300 nm) at different concentrations ranging from 0.025 to 0.1 mg/ml. After the incubation time was completed, cells were rinsed in phosphate-buffered saline solution (PBS) and fresh culture medium was added. A magnetic field (produced by a 7-A square and sine current at 1 and 10 Hz in our machine) was applied for 30 min and 1 h to the cell cultures. The

culture medium was then collected and the LDH released to the medium was quantified using the cytotoxicity detection kit (Roche), following the manufacturer's instructions. Briefly, culture supernatants were collected and centrifuged at 1000 rpm for 5 min to remove cells. Cell-free supernatants were incubated with the kit's substrate mixture. LDH activity was determined in a coupled enzymatic reaction; during this reaction, the tetrazolium salt is reduced to formazan. The formazan dye was quantified spectrophotometrically at 490 nm. Cells not exposed to our machine, with or without MMPs, were used as controls. LDH activity present in the medium was expressed as a percentage of the maximum activity, considering 100% LDH activity released to the medium as the absorbance obtained when control cells were lysed with 0.2% Triton X-100.

Intracellular localization of MMPs

Cellular interactions with microparticles were evaluated using flow cytometry and fluorescence microscopy.

Flow cytometry was used to measure changes in light scatter after the incubation of 3T3 cells with 2-μm MMPs at a concentration of 0.1 mg/ml for different incubation times.

3T3 cells were seeded in P24 multiwell plates at a density of 2.5×10^4 cells/cm^2 and incubated with particles of 2 μm at a concentration of 0.1 mg/ml for 3, 6, 12, and 24 h. Then, cells were rinsed with PBS to eliminate excess MMPs, removed by incubation with trypsin for 5 min at 37 °C and rinsed with PBS. A BD FACSCalibur™ flow cytometer containing a 488 nm laser and photomultiplier tube SSC detector was used in this study. Because the flow rate affects these measurements, they were always performed at low flow rates. The cytometer was set up to measure SSC linearly.

To determine the intracellular location of MMPs using fluorescence microscopy, 3T3 cells were seeded on coverslips at a density of 2.5×10^4 cells/cm^2 and incubated in culture medium with 2-μm particles at a concentration of 0.05 mg/ml for 24 h. Then, cells were rinsed with PBS to eliminate excess MMPs and fixed with paraformaldehyde (PFA, Merck) at a concentration of 4% in 0.1 M phosphate buffer at pH 7.4, for 30 min at room temperature. After three washes in PBS, samples were blocked for 1 h with a solution of PBS containing 10% goat serum (Gibco/Life Technologies) and 0.25% Triton X-100 (Merck). Subsequently, cells were incubated overnight at 4 °C with an antibody anti-CD63 (DSHB) diluted to 1:500 in a PBS solution with 0.25% triton and 1% goat serum. After removing the solution with primary antibody and rinsing, the samples were incubated with the secondary antibody anti-mouse-Cy3 (1:500; Jackson Immunoresearch) in PBS for 30 min at room temperature. After labeling, the coverslips were washed in PBS and distilled H_2O, allowed to dry, and mounted with Mowiol (Calbiochem).

Results and discussions

In this work, we describe a new technique to produce cell death through linear motion of particles in response to the application of a specific magnetic field, which combines a permanent magnet and Maxwell coils to produce a gradient magnetic field.

Preliminary magnetization measurements

The particles' magnetic characteristics can be obtained from their hysteresis loops, Fig. 3; MNPs show little remnant magnetism unlike the MMPs, which have a greater volume and can acquire a greater magnetic force due to their greater magnetic moment (Eq. 2 and Fig. 3). With the permanent magnet used in the experiments, the particles, both MMPs and MNPs, have practically reached the magnetization saturation region.

Preliminary heating experiments

Preliminary experiments, in which the magnetic field was applied at 7 A and 1 Hz for 2 h, showed that under the same conditions, no differences in the heating curves were observed in control samples (water) and samples containing MMPs at a concentration of 0.05 mg/ml in water (Fig. 4). Moreover, the maximum temperature reached was 32 °C, which is insufficient to destroy cells by hyperthermia.

A slight increase in temperature was observed (Fig. 4) when water at 30 °C began to enter the water jacket and temperature raised from room temperature to the temperature of the water bath (from 28 to 30 °C). Subsequently, the heating produced by the Maxwell coils increased the temperature to 32 °C, a temperature at which no cell death was observed.

Several studies have investigated the effect of alternating magnetic fields applied to cells incubated with

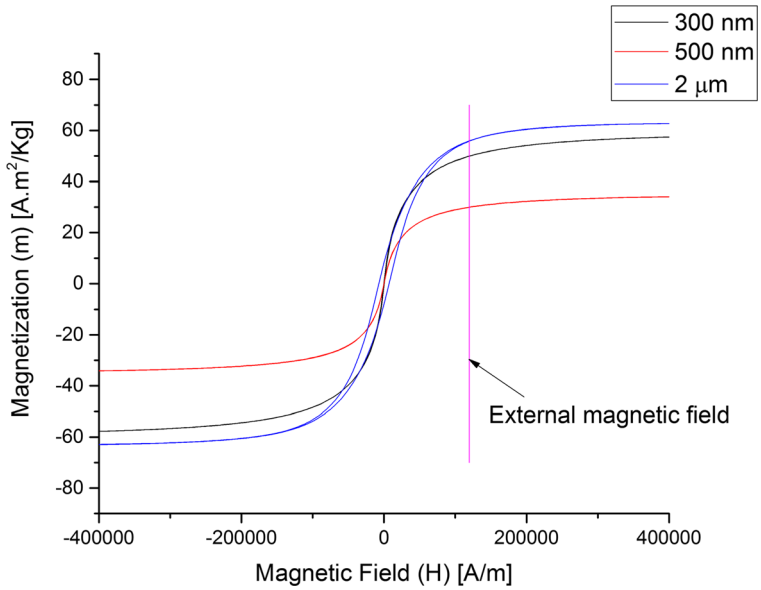

Fig. 3 Magnetization curves of the particles (300 nm, 500 nm, and 2 μm)

nanoparticles (Jordan et al. 1999; Rosensweig 2002; Creixell et al. 2011; Kumar and Mohammad 2011; Connord et al. 2015; Golovin et al. 2015). In these studies, the application of high-frequency magnetic fields produced cell death by increasing the temperature of the iron oxide nanoparticles produced through two mechanisms, referred to as Neel (caused by the movement of the magnetic moments relative to the crystal lattice structure of the single-domain MNPs) and Brown relaxations (caused by the movement of the MNPs relative to the surrounding medium) (Golovin et al. 2015). The low frequencies used did not produce any increases in temperature, in agreement with previous works (Kim et al. 2010; Zhang et al. 2014).

Intracellular localization of MMPs

Internalization of MMPs into living cells has been reported previously (Huth et al. 2004; Arbab et al. 2005; Li et al. 2008; Creixell et al. 2011; Stern et al. 2012; Domenech et al. 2013; Shen et al. 2014; Zhang et al. 2014; Yue et al. 2015; Cheng et al. 2016; Fernández-Cabada et al. 2016). To determine whether MMPs were internalized by 3T3 cells, uptake of particles by 3T3

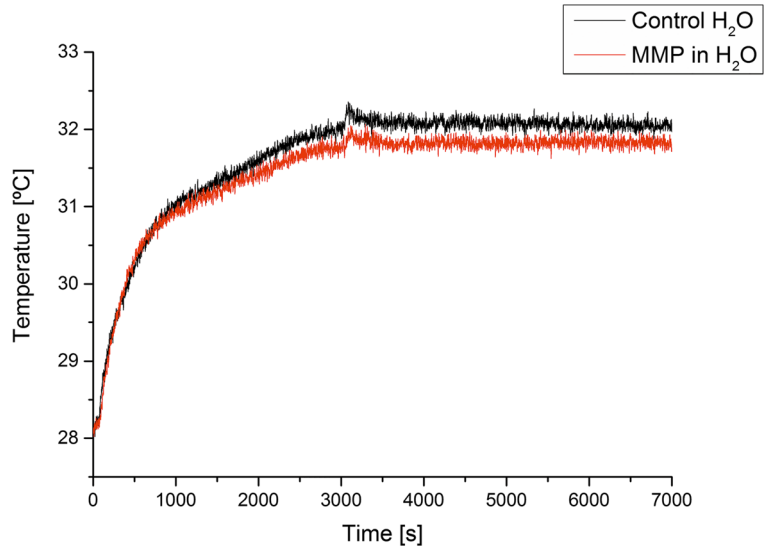

Fig. 4 The motion of the particles on the vertical axis did not produce an increase in temperature. Temperature recording in medium containing 2 μm MMPs at 0.05 mg/ml (red line) and medium alone (black line) was performed during the application of a 1-Hz magnetic field with a square-shape current of 7 A for 120 min. No significant changes in temperature were observed in both samples

cells preincubated with 2-μm MMPs was evaluated by flow cytometry after different incubation times, analyzing the variation in side scatter (SSC) intensity as an index of intracellular MMP content, as previously described (Zucker et al. 2010). Our hypothesis is that by increasing the incubation time, the SSC intensity would increase because more MMPs would be internalized within the cell. In fact, the results showed a monotonic increase in mean intensity of SSC with increasing incubation time, indicating a high uptake of MMPs by 3T3 cells at longer incubation times (Fig. 5 and Table 1).

To determine the final intracellular localization of the MNPs, a fluorescent antibody specific for lysosomes (CD63) was used. When 3T3 cells were incubated with MMPs with a size of 2 μm for 24 h, most of the particles were internalized by the cells and accumulated in intracellular vesicles, specifically in lysosomes, as determined by immunocytochemistry using a specific fluorescent antibody to label lysosomes. As we can see in Fig. 6, the presence of MMPs, visualized under light transmission as black marks, showed a strong colocalization with the fluorescent lysosome marker, indicating that most of the MMPs were stored in the cells inside these organelles.

Internalization of MMPs into living cells is normally carried out by endocytosis and macropinocytosis processes (Pouliquen et al. 1991; Arbab et al. 2005; Gupta and Gupta 2005; Li et al. 2008; Yang and Ma 2010; Canton and Battaglia 2012; Stern et al. 2012; Yanes et al. 2013), with MMPs eventually deposited in lysosomes (Huth et al. 2004; Arbab et al. 2005; Li et al. 2008; Creixell et al. 2011; Stern et al. 2012; Domenech et al. 2013; Shen et al. 2014; Zhang et al. 2014; Yue et al. 2015; Cheng et al. 2016). We have evaluated the endocytosis of the MMPs by 3T3 cells after several incubation times and showed that MMPs were progressively internalized by 3T3 cells in a time-dependent manner (Fig. 5). The high colocalization of MMPs and lysosomes (Fig. 6) indicated that MMPs were preferentially accumulated in lysosomes. Therefore, in this work, we have established the optimal conditions to target the MMPs at lysosomes without the need for an additional functionalization to target magnetic MMPs at these specific intracellular compartments.

Table 1 Mean side scatter (SSC) changes

Incubation time	Geometric mean	Ratio (treated/control)
Control	291	1
3 h	377.5	1.30
6 h	384	1.32
12 h	395	1.36
24 h	425.25	1.46

Mean side scatter (SSC) changes measured by flow cytometer in 3T3 cells treated with MMPs (2 μm) at a concentration of 0.1 mg/ml for different incubation times (3, 6, 12, and 24 h)

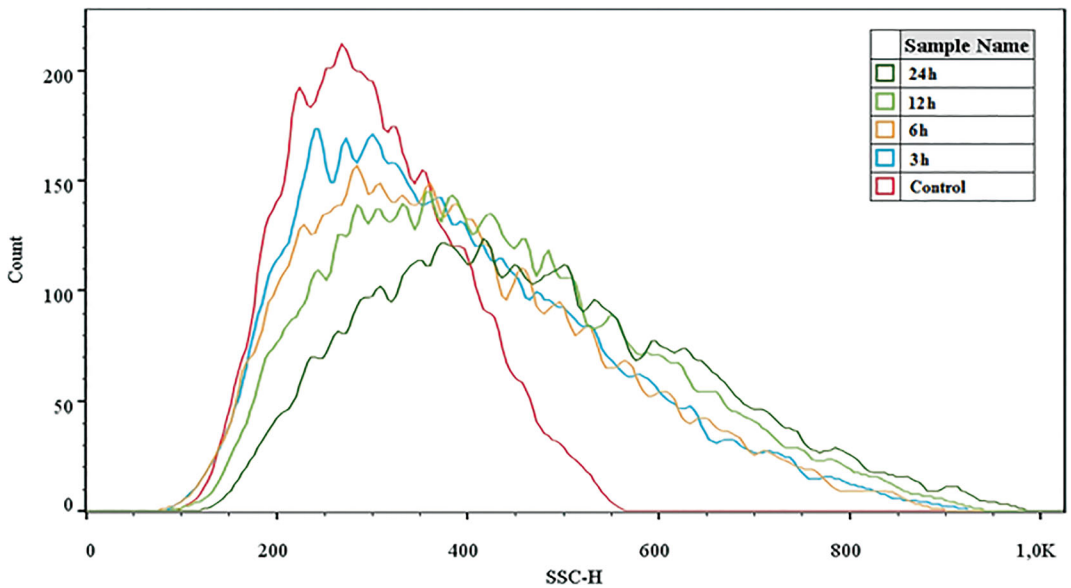

Fig. 5 3T3 cells were incubated with MMPs 2 μm in diameter at a concentration of 0.1 mg/ml for 3, 6, 12, and 24 h. SSC intensity was measured by flow cytometry. The SSC (lineal scale) increased as the incubation time increased from 3 to 24 h

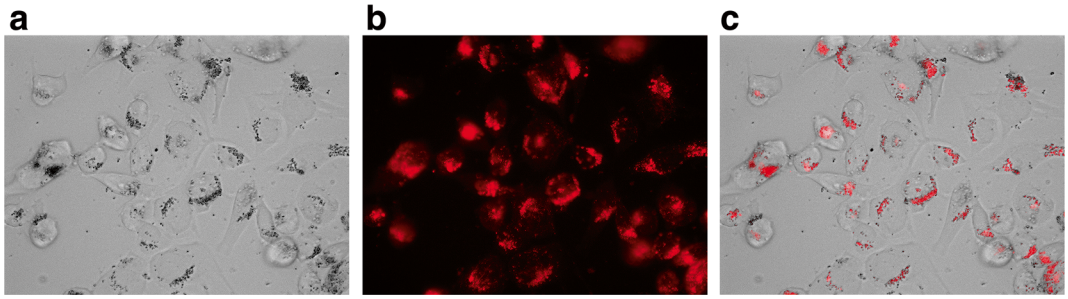

Fig. 6 Intracellular location of MMPs on 3T3 cells. 3T3 cells were incubated with MMPs (2 μm) at a concentration of 0.025 mg/ml for 24 h. MMPs are shown in transmission light (**a**). After fixation, cells were stained with an anti-CD63 to mark the lysosomes in red (**b**). A high colocalization of MMPs and lysosomes can be visualized (**c**)

Effects of magnetic field stimulation on cells incubated with MMPs

The application of a magnetic field gradient in a uniform magnetic field in our machine produces a linear movement of the MMPs (Eq. 2 and Movie 1) promoting a mechanical injury in the MMP-loaded cells in response to the movements triggered in the particles by the alternating magnetic field produced by coils and the uniform magnetic field. To determine whether the application of a magnetic field could induce cell death in these 3T3 cells previously loaded with the MMPs, magnetic fields of 1 and 10 Hz were applied under different conditions to establish the optimal parameters to achieve the maximum percentage of dead cells.

As the internalization of particles by 3T3 cells increases with longer incubation times (Fig. 5 and Table 1), we explored the effect of the incubation time of the particles on cell viability after the application of the magnetic field. Cells were preincubated with 2-μm MMPs for 3, 6, 12, and 24 h before applying 1- and 10-Hz magnetic fields to find out whether a longer incubation time could increase the cell death rate in response to the magnetic field. Indeed, longer preincubation times of particles with 3T3 cells produced higher rates of cell death after application of the magnetic field at frequencies of both 1 and 10 Hz (Fig. 7). No significant differences in cell death were observed when 3T3 cells were incubated with the particles for 12 or 24 h at 1 Hz when magnetic fields were applied. Thus, no extended periods of incubation were tested. Interestingly, when cells were preincubated with the 2-μm MMPs for 6 and 12 h and then subjected to a 10 Hz magnetic field, the rates of cell death obtained were exactly the same as those obtained at 1 Hz after preincubating the cells with the particles for half of the time (3 and 6 h, respectively). Magnetic field application at 1 Hz was in all cases significantly more efficient in triggering cell death than application at 10 Hz. Moreover, the application of the magnetic field in the absence of MMPs did not induce a significant increase in cell death in 3T3 cells, indicating a lack of toxicity of the treatments when magnetic particles were not present. Similarly, incubation of 3T3 cells with 2-μm MMPs without the application of a magnetic field did not impair cell viability at the dose and incubation times tested.

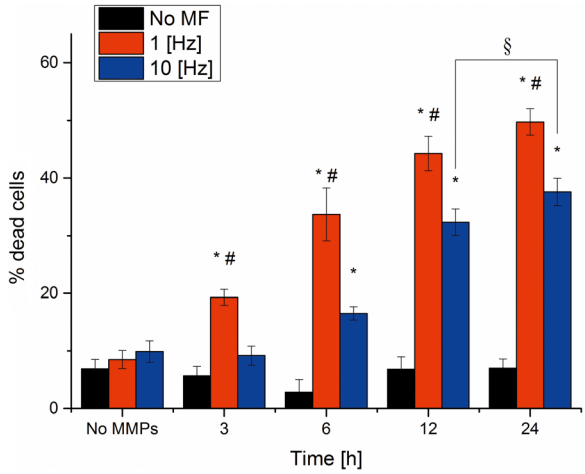

Fig. 7 Viability of 3T3 cells incubated with magnetic particles of 2 μm at a concentration of 0.1 mg/ml during different periods of time ranging from 3 to 24 h, and exposed to magnetic field treatments controlled by a square current of 7 A and frequencies of 1 and 10 Hz for 60 min. Control cells were included in all experiments: cells preincubated with particles with no magnetic field application (no MF) and cells exposed to magnetic fields at 1 and 10 Hz in the absence of MMPs (no MMPs). Data represent the mean ± S.D. of three independent experiments. ANOVA, post hoc Tukey's honest significant difference test; $*p < 0.05$, versus their respective controls: cells with no particles and no magnetic field exposure (no MF); $\#p < 0.05$, 1 versus 10 Hz; $\S p < 0.05$, 12 versus 24 h at 10 Hz

MMPs commonly accumulate in intracellular vesicles in proportion to their extracellular concentration (Huth et al. 2004; Arbab et al. 2005; Li et al. 2008; Yang and Ma 2010; Creixell et al. 2011; Canton and Battaglia 2012; Stern et al. 2012; Domenech et al. 2013; Shen et al. 2014; Zhang et al. 2014; Yue et al. 2015; Cheng et al. 2016). According to the results shown in Fig. 7, the number of dead cells increased when longer incubation times of the MMPs with 3T3 cells before the magnetic field application were tested. Therefore, the cell death rates increased when the number of MMPs inside cells was higher, as demonstrated by flow cytometry analyses (Fig. 5). The effect of the increment of MMPs concentration on cell death was also tested to determine whether higher concentrations of MMPs induced an increase in the percentage of dead cells (Fig. 8). From the results obtained, it can be seen that the percentage of dead cells is proportional to the particle concentration after the magnetic field application at frequencies of both 1 and 10 Hz. The application of the magnetic field at 1 Hz at any of the particle concentrations tested produced significantly elevated cell death rates compared to the application of a magnetic field at 10 Hz (Fig. 8), similarly to the results shown in Fig. 7.

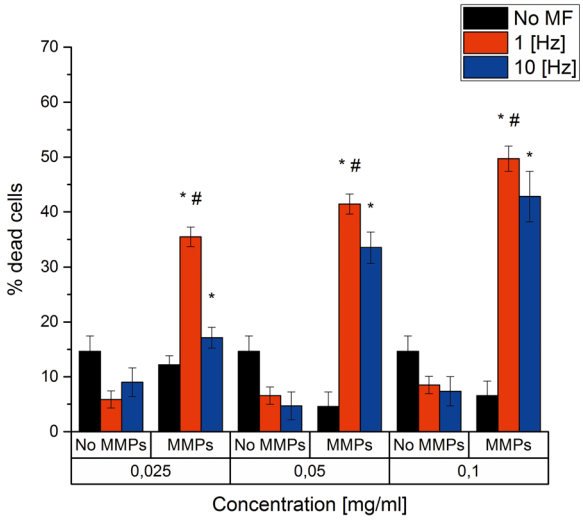

Fig. 8 Viability of 3T3 cells preincubated with magnetic particles of 2 μm at different concentrations (0.025, 0.05, and 0.1 mg/ml) for 24 h and exposed to a magnetic field of 7 A and 1 and 10 Hz. Control cells were included in all experiments: cells preincubated with particles but without application of a magnetic field (no MF) and cells exposed to magnetic fields in the absence of MMPs (no MMPs). Data represent the mean ± S.D. of three independent experiments. ANOVA, post hoc Tukey's honest significant difference test; $*p < 0.05$, versus their respective controls: cells with no particles and no MF; $\#p < 0.05$, 1 versus 10 Hz

Moreover, the concentration of the particles tested did not seem to affect the cells' viability in the absence of a magnetic field (Fig. 8). Additionally, if required, the particle concentration can be diminished by applying the right frequency (1 Hz in this case, using 2-μm particles) to obtain similar rates of cell death after the magnetic field application. This result indicated that in the case of cell toxicity in response to a high concentration of particles, the cell death could be modulated by tuning the frequency of the magnetic field. As can be seen in Fig. 8, the percentages of dead cells obtained when cells were subjected to a 10-Hz magnetic field were similar to those obtained when cells were preincubated with half the dose of particles and subjected to a 1-Hz magnetic field.

The accumulation of MMPs inside lysosomes can be relevant for inducing cell death by disrupting the lysosome membranes after the application of the magnetic field (Cheng et al. 2016). The linear motion of MMPs inside lysosomes could destabilize their membranes, promoting cell death. This fact could be very interesting for inducing cell death in tumor cells. Change in cell stiffness is a characteristic of cancer cells that affects the way they spread. It has been reported that the cell stiffness of metastatic cancer cells are more than 70% softer than the benign cells (Cross et al. 2007). Thus, the linear motion of MMPs inside lysosomes could destabilize their membranes, promoting cell death mainly in metastatic cancer cells (Hildebrandt et al. 2002).

The application of 1- and 10-Hz magnetic fields to 3T3 cells preincubated with MMPs for 24 h resulted in high cell death rates. The percentages of dead cells were higher when MMPs were incubated with 3T3 cells for longer periods before the exposure to the magnetic field (Fig. 7), indicating that when a large number of MMPs were internalized by the cells, higher cell death rates were obtained. Similarly, the percentage of dead cells increased when using higher MMP concentrations (Fig. 8), probably due to the greater magnetic force produced by the higher number of MMPs inside the cells (Jiles 1998; Serantes et al. 2014).

In order to analyze the effect of duration of exposure to the magnetic field on cell death, 3T3 cells preincubated with 2-μm MMPs for 24 h were exposed to magnetic field treatments at 1 and 10 Hz for 30 and 60 min. The percentage of dead cells obtained (Fig. 9) showed a significant increase when cells were exposed to the magnetic fields for 60 min compared to 30 min at both 1 and 10 Hz. We chose 60 min as the duration of

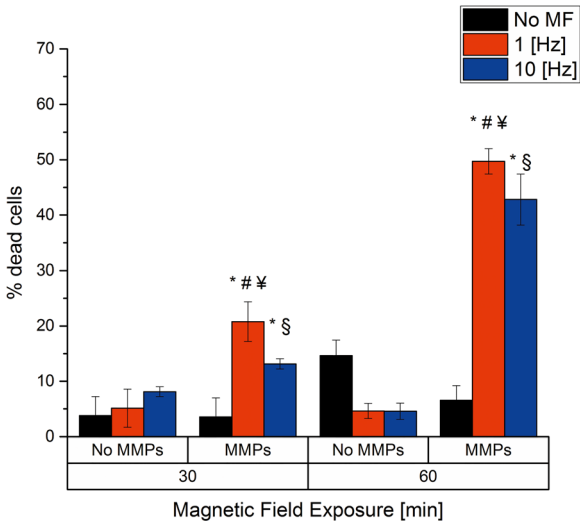

Fig. 9 Viability of 3T3 cells subjected to a square-wave magnetic field of 7 A at 1 and 10 Hz for 30 and 60 min. Cells were preincubated with magnetic particles of 2 μm at a concentration of 0.1 mg/ml for 24 h. Control cells were included in all experiments: cells preincubated with particles but without application of a magnetic field (no MF) and cells with application of a magnetic field for 30 and 60 min in the absence of MMPs (no MMPs). Data represent the mean ± S.D. of three independent experiments. ANOVA, post hoc Tukey's honest significant difference test; $*p < 0.05$, versus their respective controls: cells with no particles and no MF; $\#p < 0.05$, 1 versus 10 Hz; $¥p < 0.05$, between different magnetic field exposure times at 1 Hz; $§p < 0.05$, between different magnetic field exposures at 10 Hz

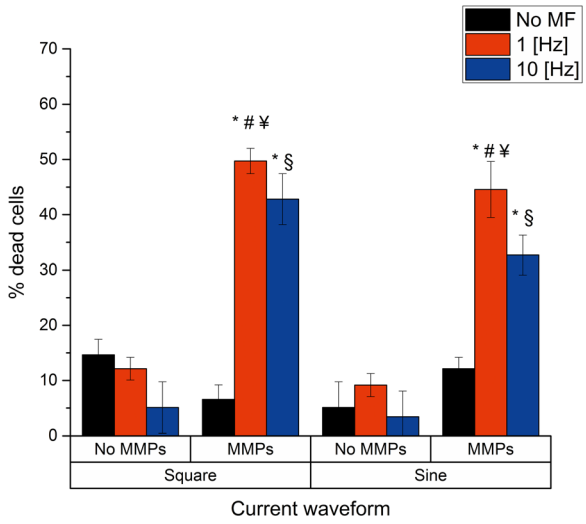

Fig. 10 Viability of 3T3 cells exposed to square-wave and sine-wave magnetic fields of 7 A at 1 and 10 Hz for 60 min. Cells were preincubated with magnetic particles of 2 μm at a concentration of 0.1 mg/ml for 24 h. Control cells were included in all experiments: cells preincubated with particles but without application of a magnetic field (no MF) and cells irradiated with a square-wave and sine-wave in the absence of MMPs (no MMPs). Data represent the mean ± S.D. of three independent experiments. ANOVA, post hoc Tukey's honest significant difference test; $*p < 0.05$, versus their respective controls: cells with no particles and no MF; $\#p < 0.05$, 1 versus 10 Hz; $¥p < 0.05$, between waveforms at 1 Hz; $§p < 0.05$ between waveforms at 10 Hz

application of magnetic field treatments in order to obtain an elevated rate of cell death.

To determine the influence of the waveform of the applied magnetic field on cell death rates, 3T3 cells preincubated with the 2-μm particles were subjected to square-wave and sine-wave magnetic fields at both frequencies 1 and 10 Hz. The results showed an increase in the rate of cell death when square-wave magnetic fields were applied (Fig. 10). The square wave produces a greater cell death rate than a sinusoidal wave because in our experimental setup, the magnetic field gradient depends on the current flowing through the Maxwell coils according to Ampere's law. So, the magnitude of the current flowing through the Maxwell coils is proportional to the magnetic field gradient (online resource 1). In addition, the magnetic force is proportional to the magnetic field gradient (Eq. 2); for that reason, the current waveform flowing through the coils Maxwell is equal to the magnetic force waveform. Thus, a square current produces a square magnetic force, and since a square wave has two maximum values of opposite sign, it means that the magnetic force has two maximum values with opposite sign while a sinusoidal current produce a sine-wave magnetic force in the vertical direction.

Once it was determined that the waveform of the magnetic field applied to cells loaded with MMPs produced significant alterations in cell death rates, we decided to determine the influence of the particle size on cell death rates after the application of the magnetic field. For this purpose, 3T3 cells were preincubated with 2 μm, 500 nm, and 300 nm MNPs at a concentration of 0.1 mg/ml for 24 h. Subsequently, cells were exposed to 1 and 10 Hz square-wave magnetic fields for 60 min and the number of dead cells was determined. The results obtained showed a significant increase in cell death rates when 3T3 cells were preincubated with 2-μm particles and subjected to the magnetic field treatments, and it was found that 1 Hz was the most effective frequency for inducing cell death (Fig. 11). However, no significant cell death could be observed after the magnetic field application when 3T3 cells were preincubated with 0.5- and 0.3-μm particles, indicating that the size of the particles is a critical parameter to induce cell death in response to the application of a gradient magnetic field.

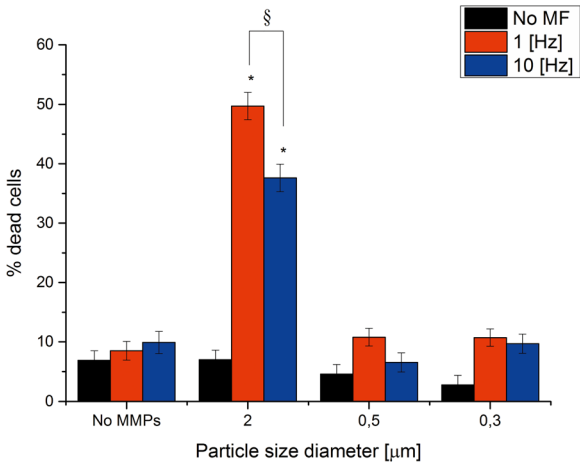

Fig. 11 Viability of 3T3 cells preincubated with MMPs of different sizes (2, 0.5, and 0.3 μm) at a concentration of 0.1 mg/ml for 24 h and exposed to magnetic fields of 7 A and 1 and 10 Hz for 60 min. The graph also shows the basal cell death in control cells, cells without magnetic field application (no MF), and cells irradiated in the absence of MMPs (no MMPs). Data represent the mean ± S.D. of three independent experiments. ANOVA, post hoc Tukey's honest significant difference test; $*p < 0.05$, versus their respective controls: cells with no particles and no MF, $§p < 0.05$ between 1 and 10 Hz

Due to their size, MMPs that are 2 μm in diameter are ferromagnetic, meaning they have more magnetic domains than MNPs (Guimarães 2009), and thus MMPs acquiring greater magnetization from an external permanent magnet, and acquiring greater momentum in our machine (Eq. 2, Fig. 3 and Table 2), produce more mechanical cell damage than MNPs (Fig. 11). We obtained a higher rate of cell death when using 2 μm MMPs than when using MNPs.

Alternating magnetic fields with a frequency below 0.1 MHz, which can penetrate tissues (> 1 m), and small magnetic fields ($B < 1$ T), are considered safe and negligible for biological applications (Golovin et al. 2015). In this work, we have used a permanent magnet of 100 mT, which did not alter cell viability by itself, and

Table 2 Magnetic force produced by a particle

Microparticle diameter [μm]	Force [N]
2	1.33×10^{-13}
0.5	6.08×10^{-16}
0.3	2.22×10^{-16}

Magnetic force produced by a particle in the vacuum due to the magnetic arrangement of our equipment when circulating a current of 7 A (Eq. 2)

frequencies of 1 and 10 Hz to avoid interaction with biological processes, obtaining higher cell death rates when applying the lower frequency (1 Hz) in all tested conditions. These results are consistent with previous data (Kim et al. 2010) obtaining a reduced cell viability with low frequencies attributed to a decrease in particles oscillation amplitude at higher frequencies.

Studies cell death triggered by the rotation of nanoparticles is promoted in response to the application of low-frequency magnetic fields (Zhang et al. 2014; Golovin et al. 2015; Yue et al. 2015; Cheng et al. 2016). In this case, the rotation speed of nanoparticles depends on dynamic magnetic fields (dmf) (Zhang et al. 2014). A similar technique was used with microdiscs, where a magnetic field with low frequency created magnetic-vortex microdiscs to produce cell death (Kim et al. 2010; Cheng et al. 2016) (Leulmi et al. 2015) achieved cell death in cancer cells through microdisks using magnetic stimulation AC; our equipment achieves cell death through a linear movement with spherical MMPs at low frequencies produced by Maxwell coil, which is powered by an AC current, and a uniform magnetic field.

A permanent magnetic field produces a cluster of microparticles, since each particle changes the magnetic field because the gradient around it loses ideal homogeneity (Mathieu and Martel 2007; Mathieu and Martel 2009; Hamad Farah 2016). The microparticle cluster can be dispersed by withdrawing the external magnetic field, a procedure that has been verified several times in our laboratory. In addition, the magnetic field produced by the permanent magnet is greater than the magnetic field produced by the Maxwell coils, which can be considered negligible, so the particles have a behavior as if they were inside of a 100-mT uniform magnetic field (Mathieu and Martel 2010). In addition, commercial particles have been subjected to magnetic fields of 800 mT for extended periods of time without showing alterations in their composition, probably due to the coating layer that gives protection to the iron core and does not cause toxicity (Laconte et al. 2005; Hamad Farah 2016).

Liu et al. move MNPs using magnetic field gradients, but as the magnetic moment of the MNP depends on the external magnetic field, which varies depending on the position of the MNP, the magnetic force is not constant (Liu et al. 2015). Nothnagel et al. moved a single body of ferromagnetic material using a magnetic particle imaging (MPI) system, but the gradient of the magnetic

field was obtained through permanent magnets and the homogeneous magnetic field was produced through coils (Nothnagel et al. 2016). On the contrary, our equipment, which is capable of moving several microparticles, uses a permanent magnet whose magnetic field strength (100 mT) is much greater than the magnetic field strength produced by the Maxwell coil (5.3 mT); in this case, the magnetic moment of the MMPs is constant. In addition, a constant magnetic field gradient is produced by the Maxwell coils to obtain a constant magnetic force (see Movie 1 and Eq. 2).

Conclusions

MMPs are internalized by 3T3 cells and accumulated inside lysosomes in a time- and concentration-dependent manner. MMPs internalized by 3T3 cells are capable of producing cell death when subjected to a constant magnetic field and a uniform magnetic gradient by mechanical actions that do not produce temperature increases. We have determined that the highest cell death rates are achieved by using the larger diameter particles, probably due to the stronger magnetic force induced. Our results also demonstrate that the waveform of the applied magnetic field is critical for inducing cell death, as a square current is more efficient in eliminating cells than the sine current.

In summary, the cell death produced by the application of low-frequency magnetic fields in the presence of MMPs is caused by mechanical interactions since the slight increase in temperature observed is insufficient to produce cell damage. The device developed for the application presented here could be of future interest in the removal of tumor cells considering that the cell stiffness of metastatic cancer cells is more than 70% softer than normal cells. MMPs can also be functionalized with molecules to specifically recognize cancer cells. Biofunctionalized MMPs could be able to target cancer cells allowing their selective elimination by the application of magnetic fields of an appropriate frequency.

Acknowledgements The authors would like to thank the expert technical assistance of Soledad Martínez and the work done by Oscar Ernesto Simón Casanova Carvajal and Ana Lorena Urbano Bojorge.

Funding The authors gratefully acknowledge the financial support of the Comunidad Autónoma de Madrid (S2010-BMD-2460) to Milagros Ramos-Gómez and the financial support to Carlos Amaya Jaramillo by Secretaria de Educación Superior, Ciencia, Tecnología e Innovación (SENESCYT-Ecuador).

Compliance with ethical standards

Conflict of interest The authors declare that they have no conflict of interest.

References

Arbab AS, Wilson LB, Ashari P et al (2005) A model of lysosomal metabolism of dextran coated superparamagnetic iron oxide (SPIO) nanoparticles: implications for cellular magnetic resonance imaging. NMR Biomed 18:383–389. https://doi.org/10.1002/nbm.970

Canton I, Battaglia G (2012) Endocytosis at the nanoscale. Chem Soc Rev 41:2718. https://doi.org/10.1039/c2cs15309b

Cheng Y, Muroski ME, Petit DCMC et al (2016) Rotating magnetic field induced oscillation of magnetic particles for in vivo mechanical destruction of malignant glioma. J Control Release 223:75–84. https://doi.org/10.1016/j.jconrel.2015.12.028

Connord V, Clerc P, Hallali N et al (2015) Real-time analysis of magnetic hyperthermia experiments on living cells under a confocal microscope. Small 11:2437–2445. https://doi.org/10.1002/smll.201402669

Creixell M, Bohórquez AC, Torres-lugo M, Rinaldi C (2011) EGFR-targeted magnetic nanoparticle heaters kill cancer cells without a sensible temperature rise.SI. ACS Nano 5:3–8

Cross SE, Yu-Sheng J, Jianyu R, Gimzewski JK (2007) Nanomechanical analysis of cells from cancer patients. Nat Nanotechnol 2:780–783. https://doi.org/10.1038/nnano.2007.388

Dobson J (2006) Magnetic nanoparticles for drug delivery. Drug Dev Res 67:55–60. https://doi.org/10.1002/ddr.20067

Domenech M, Marrero-Berrios I, Torres-Lugo M, Rinaldi C (2013) Lysosomal membrane permeabilization by targeted magnetic nanoparticles in alternating magnetic fields. ACS Nano 7:5091–5101. https://doi.org/10.1021/nn4007048

Fernández-Cabada T, de Pablo CS-L, Pisarchyk L et al (2016) Optical hyperthermia using anti-epidermal growth factor receptor-conjugated gold nanorods to induce cell death in glioblastoma cell lines. J Nanosci Nanotechnol 16:7689–7695. https://doi.org/10.1166/jnn.2016.12570

Frame BR, Zhang H, Cocciolone SM et al (2000) Production of transgenic maize from bombarded type II callus: effect of gold particle size and callus morphology on transformation efficiency. Vitr Cell Dev Biol - Plant 36:21–29. https://doi.org/10.1007/s11627-000-0007-5

Golovin YI, Gribanovsky SL, Golovin DY et al (2015) Towards nanomedicines of the future: remote magneto-mechanical actuation of nanomedicines by alternating magnetic fields. J Control Release 219:43–60. https://doi.org/10.1016/j.jconrel.2015.09.038

Guimarães AP (2009) The basis of nanomagnetism. In: Avouris P, Bhushan B, Bimberg D, von Klitzing K, Sakaki H, Wiesendanger R (eds) Principles of nanomagnetism. Springer Berlin Heidelberg, Berlin, pp 1–20

Gupta AK, Gupta M (2005) Cytotoxicity suppression and cellular uptake enhancement of surface modified magnetic nanoparticles. Biomaterials 26:1565–1573. https://doi.org/10.1016/j.biomaterials.2004.05.022

Hamad Farah F (2016) Magnetic microspheres: a novel drug delivery system. J Anal. Pharm Res. 10.15406/japlr.2016.03.00067

Hergt R, Dutz S, Müller R, Zeisberger M (2006) Magnetic particle hyperthermia: nanoparticle magnetism and materials development for cancer therapy. J Phys Condens Matter 18: S2919–S2934. https://doi.org/10.1088/0953-8984/18/38/S26

Hernando Grande A (2007) Nanotecnología Y Nanopartículas Magnéticas : La. Rev la Real Acad Ciencias Exactas, Físicas y Nat 101:321–327

Hildebrandt B, Wust P, Ahlers O et al (2002) The cellular and molecular basis of hyperthermia. Crit Rev Oncol Hematol 43:33–56. https://doi.org/10.1016/S1040-8428(01)00179-2

Huth S, Lausier J, Gersting SW et al (2004) Insights into the mechanism of magnetofection using PEI-based magnetofectins for gene transfer. J Gene Med 6:923–936. https://doi.org/10.1002/jgm.577

Jiles D (1991) Magnetic measurements. In: Chapman and Hall (ed) Introduction to magnetism and magnetic materials. Springer US, Boston, pp 47–68

Jordan A, Scholz R, Wust P et al (1999) Magnetic fluid hyperthermia (MFH): cancer treatment with AC magnetic field induced excitation of biocompatible superparamagnetic nanoparticles. J Magn Magn Mater 201:413–419. https://doi.org/10.1016/S0304-8853(99)00088-8

Kim D-H, Rozhkova EA, Ulasov IV et al (2010) Biofunctionalized magnetic-vortex microdiscs for targeted cancer-cell destruction. Nat Mater 9:165–171. https://doi.org/10.1038/nmat2591

Kumar CSSR, Mohammad F (2011) Magnetic nanomaterials for hyperthermia-based therapy and controlled drug delivery. Adv Drug Deliv Rev 63:789–808. https://doi.org/10.1016/j.addr.2011.03.008

Laconte L, Nitin N, Bao G (2005) Magnetic nanoparticle probes. Mater Today 8:32–38. https://doi.org/10.1016/S1369-7021(05)00893-X

Leulmi S, Chauchet X, Morcrette M et al (2015) Triggering the apoptosis of targeted human renal cancer cells by the vibration of anisotropic magnetic particles attached to the cell membrane. Nano 7:15904–15914. https://doi.org/10.1039/C5NR03518J

Li W, Chen C, Ye C et al (2008) The translocation of fullerenic nanoparticles into lysosome via the pathway of clathrin-mediated endocytosis. Nanotechnology 19:145102. https://doi.org/10.1088/0957-4484/19/14/145102

Liu H, Sun J, Wang H et al (2015) Quantitative evaluation of the total magnetic moments of colloidal magnetic nanoparticles: a kinetics-based method. ChemPhysChem 16:1598–1602. https://doi.org/10.1002/cphc.201500093

Mathieu JB, Martel S (2007) Magnetic microparticle steering within the constraints of an MRI system: proof of concept of a novel targeting approach. Biomed Microdevices 9:801–808. https://doi.org/10.1007/s10544-007-9092-0

Mathieu JB, Martel S (2009) Aggregation of magnetic microparticles in the context of targeted therapies actuated by a magnetic resonance imaging system. J Appl Phys. https://doi.org/10.1063/1.3159645

Mathieu JB, Martel S (2010) Steering of aggregating magnetic microparticles using propulsion gradients coils in an MRI scanner. Magn Reson Med 63:1336–1345. https://doi.org/10.1002/mrm.22279

Nothnagel N, Rahmer J, Gleich B et al (2016) Steering of magnetic devices with a magnetic particle imaging system. IEEE Trans Biomed Eng 63:2286–2293. https://doi.org/10.1109/TBME.2016.2524070

Pouliquen D, Le Jeune JJ, Perdrisot R et al (1991) Iron oxide nanoparticles for use as an MRI contrast agent: pharmacokinetics and metabolism. Magn Reson Imaging 9:275–283. https://doi.org/10.1016/0730-725X(91)90412-F

Rosensweig REE (2002) Heating magnetic fluid with alternating magnetic field. J Magn Magn Mater 252:370–374. https://doi.org/10.1016/S0304-8853(02)00706-0

Sanchez S, Solovev AA, Schulze S, Schmidt OG (2011) Controlled manipulation of multiple cells using catalytic microbots. Chem Commun (Camb) 47:698–700. https://doi.org/10.1039/c0cc04126b

Serantes D, Simeonidis K, Angelakeris M et al (2014) Multiplying magnetic hyperthermia response by nanoparticle assembling. J Phys Chem C 118:5927–5934. https://doi.org/10.1021/jp410717m

Shen H, Tong S, Bao G, Wang B (2014) Structural responses of cells to intracellular magnetic force induced by superparamagnetic iron oxide nanoparticles. Phys Chem Chem Phys 16:1914–1920. https://doi.org/10.1039/c3cp51435h

Stern ST, Adiseshaiah PP, Crist RM (2012) Autophagy and lysosomal dysfunction as emerging mechanisms of nanomaterial toxicity. Part Fibre Toxicol 9:20. https://doi.org/10.1186/1743-8977-9-20

Yanes RE, Tarn D, Hwang AA et al (2013) Involvement of lysosomal Exocytosis in the excretion of mesoporous silica nanoparticles and enhancement of the drug delivery effect by exocytosis inhibition. Small 9:697–704. https://doi.org/10.1002/smll.201201811

Yang K, Ma Y-Q (2010) Computer simulation of the translocation of nanoparticles with different shapes across a lipid bilayer. Nat Nanotechnol 5:579–583. https://doi.org/10.1038/nnano.2010.141

Yue T, Zhang X, Huang F (2015) Molecular modeling of membrane responses to the adsorption of rotating nanoparticles: promoted cell uptake and mechanical membrane rupture. Soft Matter 11:456–465. https://doi.org/10.1039/C4SM01760A

Zhang E, Kircher MF, Koch M et al (2014) Dynamic magnetic fields remote-control apoptosis via nanoparticle rotation. ACS Nano 8:3192–3201. https://doi.org/10.1021/nn406302j

Zucker RM, Massaro EJ, Sanders KM et al (2010) Detection of TiO2 nanoparticles in cells by flow cytometry. Cytometry A 77:677–685. https://doi.org/10.1002/cyto.a.20927